Genetic perturbation of MAPK11 (p38β) promotes radiosensitivity by enhancing IR-associated senescence.

Fernández-Aroca DM[1±,*], García-Flores N[1±], Frost S[2], Jiménez-Suarez J[1], Rodríguez-González A[2], Fernández-Aroca P[1], Sabater S[3], Andrés I[3], Garnés-García C[1], Belandia B[4], Cimas FJ[1,5], Villar D[2], Ruiz-Hidalgo MJ[1,5], Sánchez-Prieto R[1,4*].

1. Laboratorio de Oncología Molecular, Unidad de Medicina Molecular, Centro Regional de Investigaciones Biomédicas, Universidad de Castilla-La Mancha. Unidad Asociada de Biomedicina UCLM, Unidad asociada al CSIC, Albacete, España.

2. Centre for Genomics and Child Health, Blizard Institute, Faculty of Medicine and Dentistry, Queen Mary University of London, London, UK.

3. Servicio de Oncología Radioterápica, Complejo Hospitalario Universitario de Albacete, Albacete, España

4. Departamento de Biología del Cáncer, Instituto de Investigaciones Biomédicas Alberto Sols (CSIC-UAM). Madrid, España. Unidad Asociada de Biomedicina UCLM, Unidad asociada al CSIC

5. Área de Bioquímica y Biología Molecular. Facultad de Medicina. Universidad de Castilla-La Mancha, Albacete, España.

± Both authors have contributed equally to this work

***** Both authors have contributed equally to this work

Correspondence should be addressed to:

Diego M. Fernández Aroca, Ph.D (Laboratorio de Oncología Molecular, Facultad de Medicina de Albacete, Universidad de Castilla La Mancha) diego.fernandez@uclm.es

Ricardo Sánchez Prieto, Ph.D (Instituto de Investigaciones Biomédicas de Madrid. Lab 1.5.2) rsprieto@iib.uam.es Phone 915854420.

Abstract

Background and purpose: MAPKs are among the most relevant signalling pathways involved in coordinating cell responses to different stimuli. In this group we can find p38MAPK, constituted by 4 different proteins with a high sequence homology: p38α, p38β, p38γ and p38δ. Despite the high homology, each member shows unique expression patterns and even exclusive functions. Thus, analysing protein-specific functions of MAPK members is necessary to unequivocally uncover the roles of this signalling pathway. Here, we propose to investigate the possible role of p38β (MAPK11) in the cell response to ionizing radiation (IR).

Materials and methods: We have developed MAPK11/14 knockdown through shRNA and CRISPR interference gene perturbation approaches, and analysed the implication of this MAPKs in cell response to ionizing radiation in A549, HCT-116 and MCF-7 cancer cell lines. Specifically, we analysed IR toxicity by clonogenic assays; DNA damage response activity by immunocytochemistry; apoptosis and cell cycle by flow cytometry (Annexin V and propidium iodide, respectively); DNA repair by comet assay; and senescence induction by both X-Gal staining and gene expression of senescence-associated genes by RT-qPCR.

Results: Our findings demonstrate a critical role of MAPK11 in the cellular response to IR by controlling the associated senescent phenotype, and without observable effects on DDR, apoptosis, cell cycle or DNA damage repair

Conclusion: Our results highlight MAPK11 as a novel mediator of the cellular response to ionising radiation through the control exerted onto IR-associated senescence.

Keywords

Ionizing radiation, radiosensitization, senescence, MAPK11, p38β

List of abbreviations

DDR: DNA damage response

DSB: Double strand break

gRNA: Guide RNA

IR: Ionizing radiation

MAPK: Mitogen Activated Protein Kinase

RT-qPCR: Quantitative real-time PCR

S.D.: Standard deviation

SF: Surviving fraction

shRNA: short hairpin RNA

Acknowledgments

We would like to thank the staff from the Radiotherapy Unit at the Complejo Hospitalario Universitario de Albacete for the technical support.

Introduction

Radiotherapy, applied to around 50% of cancer patients, has become a cornerstone in cancer therapy [1], being especially relevant in some types of tumours such as breast, colon or lung [2]. It is therefore essential to uncover the molecular and biological processes triggered by ionising radiation (IR) which could improve the effectiveness of treatments. Consequently, the search of mechanisms responsible for sensitisation and resistance to radiotherapy, both *de novo* and acquired, has been a long-standing issue in radiobiology [3–6]. Several signalling pathways [7], biological processes [8,9], genetic alterations [10,11], and even epigenetic elements [12] have been related to the cellular response to IR, however, we still do not have a complete picture of the molecular elements involved in this biological response that could contribute to improve and personalise radiotherapy.

Among the variety of signalling pathways implicated in the cellular response to IR, classic MAPK pathways are among the most relevant. The implication of some MAPK signalling pathways in response to IR have also been interrogated: ERK1/2 have been related to resistance [13,14]; JNK have been linked to ATM and DNA damage response [15–19]; ERK5 has also been related to ATM-mediated signalling pathway and IR-induced DNA damage repair [20,21]. Our work focuses on p38MAPK, which has been extensively studied in response to different types of cellular stress [22,23], including IR [24–26].

Within p38MAPK family, four proteins with high homology can be found: p38α (MAPK14), p38β (MAPK11), p38γ (MAPK12) and p38δ (MAPK13). With the term p38MAPK we will refer to all four proteins. Despite these members sharing around 60% sequence homology [27], each of them shows not just different tissue expression patterns [28,29] but also specific functions in different biological processes such as myocyte differentiation [30], female cancers [31] or inflammation [32]. In addition, even opposite roles for each member have been described [33] (e.g. in activating AP-1-dependent transcription in breast cancer cell lines [34]). Most of the current evidence linking p38MAPK and cancer are focused onto MAPK14, due to its ubiquitous and abundant expression [35]. However, a growing body of evidence support a key role in cancer for other members of the family, such as MAPK12 and MAPK13 [36,37]. Indeed, recent evidence indicates important roles for MAPK11 in cancer and its therapy [38]. In addition, it is noteworthy that the vast majority of publications assessing p38MAPK roles are based on pharmacological approaches, which at best allow to distinguish MAPK11/14 from MAPK12/13 not addressing protein-specific functions.

Nonetheless, p38MAPK signalling pathway has been linked with the response to DNA damage and, specifically, to IR. TAO kinases are able to activate p38MAPK through ATM/ATR pathways in response to IR [41,42], emerging as regulators of p38-mediated response to DNA damage [41]. It is also remarkable that p38MAPK have been found to be critical in the signal transduction triggered by IR, being required for activation of other key processes (e.g. IR-induced apoptosis [43] and protein activation such as AKT [44]).

Among the p38MAPK proteins which have been specifically proposed as mediators of cell response to IR, MAPK12 have been identified as a key protein involved in mediating IR-induced cell cycle arrest [25]. In addition, recent evidence indicated MAPK11, but not MAPK14, could have a relevant role in the radiosensitising effect of gemcitabine [45].

Against this background, we aimed to clarify the specific role of MAPK11 in the cellular response to radiotherapy and its potential as mediator of the cellular response to DNA damage in different *in vitro* experimental models, including colon, lung and breast cancer cell lines.

Materials and Methods:

Cell lines and plasmids

A549 (Lung cancer), HCT-116 (Colon cancer) and HEK293T were purchased from ATCC. The breast cancer cell line MCF-7 was kindly provided by Dr. Alberto Ocaña (Translational Research Unit, Complejo Hospitalario Universitario de Albacete, Spain). Cells were maintained in 5% CO_2 and 37°C; and grown in Dulbecco's modified Eagle's medium supplemented with 10% fetal bovine serum, 1% glutamine and 1% Penicillin/Streptomycin. All cell culture reagents were provided by Lonza.

Plasmids used for shRNA interference (Sigma-Aldrich) were as follows: Human pLKO.1-puro-shRNAMAPK14 (Sigma SHCLNG-NM_001315; TRCN0000000511), Human pLKO.1-puro-shRNAMAPK11 (Sigma SHCLNG-NM_002751; (TRCN0000199694), and pLKO.1-puro empty vector (Sigma SHC001).

Plasmids used for CRISPR interference (CRISPRi) were as follows: TRE-dCas9-KRAB-IRES-GFP (Addgene #85556) [44], pU6-sgRNA-puro-BFP (Addgene #60955) [45].

Transfections and infections

Lentiviral production and cell infection were performed as previously described [46,47].

Inducible CRISPR interference (CRISPRi)

A549 cells were infected with lentiviruses containing TRE-dCas9-KRAB-IRES-GFP [48], treated for 4 days with 1 µg/ml doxycycline and then GFP-positive cells were sorted by flow cytometry. Next, dCas9-expressing cells were infected with pU6 plasmids harbouring non-target control (NTC) or sgMAPK11 gRNAs and selected with 1µg/ml puromycin for 3 days. To achieve full dCas9 expression, cells were treated with 1 µg/ml doxycycline 5 days prior to cell seeding and maintained over the course of the experiments.

gRNAs (Supplementary Table 1) were designed with CHOPCHOP [49], purchased from IDT (Integrated DNA Technologies), and cloned into pU6-sgRNA-puro-BFP as previously described [50].

Western Blotting

Cells were collected in lysis buffer (100 mM HEPES, pH 7.5, 50 mM NaCl, 0,1% Triton X-100, 5 mM EDTA, 0,125 M EGTA). Protease and phosphatase inhibitors (Sigma-Aldrich) were added prior to lysis. Protein quantification was performed by using the BCA Protein Assay Kit (ThermoFisher) following the manufacturer's instructions. Indicated amounts of protein were loaded onto appropriate percentage SDS-PAGE, transferred to PVDF membranes using semi-dry Pierce Power Blot (ThermoFisher) and blotted against different proteins via specific antibodies (Supplementary Table 2).

Antibodies were detected by enhanced chemiluminescence (Amersham) in a LAS-3000 system (FujiFilm). Images show a representative experiment out of three with similar results.

Immunocytochemistry

Cells were grown onto SPL cell culture slides (Labclinic) 24 h prior to irradiation. After treatment cells were fixed, permeabilized and incubated with the indicated antibodies (Suplementary Table 2) as previously described [51]. Positive immuno-fluorescence was detected using a Zeiss Apotome fluorescence microscope and processed using Zen 2009 Light Edition program (Zeiss). Foci quantification was performed with CellProfiler (Broad) [52]. Images show a representative cell from a minimum of 100 quantified (5 fields per sample captured). Data shown are the average of, at least, three independent experiments.

RNA isolation, reverse transcription and Real-time Quantitative PCR

Total RNA was obtained as previously described [53]. cDNA synthesis was performed with RevertAid First Strand cDNA synthesis Kit (Thermo Scientific) following manufacturer's protocol in an iCycler thermal cycler (Biorad). Real time PCR was performed with Fast SYBR Green Master kit (Thermo Scientific) in a 7500 Fast Real-Time PCR instrument (Applied Byosystems). PCR conditions were as previously described [53]. Primers for all target sequences were designed by using NCBI BLAST software and purchased from Merck as DNA oligos. Primer sequences can be found in Supplementary Table 1. Data shown are the average of, at least, three independent experiments performed in triplicate.

Irradiation and clonogenic assays

Cells were irradiated by the technical staff of Radiotherapy Unit at University General Hospital of Albacete, in a Clinac Low Energy 600C linear electron accelerator from Varian (Palo Alto, California, USA) at a dose rate of 600 cGy/min in a radiation field of 40x40 cm. Clonogenic assays were performed as previously described [53,54]. Plates were photographed and colonies were counted with the ImageJ plugin "Cell counter". Colonies with less than 5 mm diameter were discarded. Values were referred to unirradiated

controls, set at 1. SF2Gy was calculated by applying a linear-quadratic model [55]. Data shown are the average of, at least, three independent experiments performed in triplicated cultures.

Beta-galactosidase activity

Six days after irradiation, cells were washed in PBS, fixed for 5 min (room temperature) in 12% formalin, washed twice for 5 minutes, and incubated for 16 h at 37°C (no CO_2) with fresh SA-β-Gal staining [56]. Images were acquired at 10x using Zeiss Apotome. Images show a representative field out of 5 captured per sample (minimum of 100 cells quantified per condition). Data shown are the average of three independent experiments.

Flow cytometry

For cell cycle analysis, 10^4 cells were seeded in 6 cm plates 24 hours prior to irradiation and cell cycle was analysed as previously described at indicated times [57]. For apoptosis detection, 10^5 cells were seeded in 6 cm plates, 24 h later cells were treated with IR and after 48 h apoptosis was detected with Annexin V-FITC (Immunostep) following manufacturer's instructions.

Samples were processed in a MACSQuant Analyzer 10 (Miltenyi Biotec). Data were analysed by using FlowingSoftware (University of Turku). Data shown are the average of, at least, three independent experiments performed.

Comet Assay

DNA fragmentation and repair was measured with the alkaline comet assay [58] by seeding 10^5 cells in 6 cm plates 24 hours prior to irradiation. After treatment, cells were harvested, centrifuged, resuspended in 0.7% low melting point agarose and added to 1% agarose pre-coated microscope slides. Next, slides were immersed in 50 mL of fresh pre-chilled alkaline lysis solution containing 10mM Trizma base, 2.5M NaCl, 0.1% Triton X-100, 100mM Na_2EDTA (pH=11) and incubated overnight at 4 °C in darkness. Lysis solution was removed, the slides were transferred to 50 mL of fresh alkaline electrophoresis solution (300mM NaOH, 1 mmol/L EDTA, pH > 12) and incubated at room temperature for 10 min. Then, electrophoresis was performed in a horizontal electrophoresis tank (Bio-Rad) pre-filled with electrophoresis solution at 25 V for 20 min. Slides were then rinsed with PBS and stained 5 min at 4 °C with 10 μg/μl propidium iodide (Cell signalling). Images were acquired at 10x magnification using Zeiss Apotome fluorescence microscope and analysed with the plugin OpenComet [59] (ImageJ) to measure tail moment (DNA% in tail * tail length). Data shown are the average of three independent experiments.

Cell proliferation measurements

For cell proliferation measurements, 10^4 cells/well were seeded in 24-well plates and proliferation was analysed at 1, 2 and 3 days later by an MTT-based assay as previously described [43]. Data shown are the average of three independent experiments performed in triplicated cultures.

Statistical analysis

Data are presented as mean ± standard deviation (S.D). Statistical significance was evaluated by Student's t test or ANOVA using GraphPad Prism v9.0 software. The statistical significance of differences is indicated in figures by asterisks as follows: *$p < 0.05$, **$p < 0.01$ and ***$p<0.001$.

For Kaplan-Meyer curves, analysis was performed in cBioportal [60] by using curated TCGA Breast Cancer dataset. The differences between survival curves were examined using the log-rank test. Patients were segregated depending on MAPK11 mRNA levels.

Results

Given the evidence of p38MAPK implication in the cellular response to IR, we first aimed to interrogate the specific role of MAPK11 and MAPK14, the two highly and ubiquitously expressed members of p38MAPK across A549 (lung), HCT-116 (colon) and MCF-7 (breast) cancer cells lines. After achieving an effective MAPK14 or MAPK11 knockdown by shRNA (Fig. 1A, D, G and Sup. Fig. 1), we analysed viability after IR exposure by 15-days clonogenic assays. We did not observe a significant effect upon MAPK14 abrogation in any of the cell lines tested, however, knockdown of MAPK11 led to a significant reduction in cell survival after IR exposure (Fig. 1B, E, H)) in all three cell lines, but did not affect proliferation in the absence of radiation (Sup. Fig. 2). Indeed, SF2Gy showed a marked and specific decrease upon MAPK11 ablation (Fig. 1C, F, I), suggesting a potential role for this MAPK in radiobiology.

Since the activity of DNA Damage Response (DDR) is one of the most important cell pathways activated in response to IR, we next investigated whether MAPK11 plays any role in this signalling pathway by choosing as experimental model the A549 cell line. To this end, we analysed activation of key molecules in the cellular response to DNA damage, such as ATM and homologous-recombination repair mediator BRCA1. These experiments showed no differences in the number of pATM/pBRCA1 foci per nuclei in cells with reduced MAPK11 expression compared to E.V. (Fig. 2A). This result was also confirmed by comet assay, in which no differences in DNA repair capacity were found (Fig 2. B). Furthermore, we confirmed these results in MCF-7 and HCT-116 cell lines (Sup. Fig. 3), thus concluding MAPK11 does not play a direct role in mediating DDR activity.

Next, we studied MAPK11 effects in terms of IR-associated cell cycle blockage and apoptosis induction, as these are other two relevant, early cellular responses to DNA damage. We did not observe MAPK11 to have a determinant role onto G2/M cell cycle phase accumulation 24 h after treatment with radiotherapy in A549 cells (Fig. 3A). Interestingly, we observed a slight but non-significant premature release from G2/M blockage in shMAPK11 cells 48 h after IR. Regarding IR-induced apoptosis, we did not find significant differences in induction of apoptosis 48h after IR exposure in A549 (Fig 3B), HCT-116 or MCF-7 cell lines (Sup. 3). Therefore, the collective evidence from these experiments discards a direct role of MAPK11 in the early cellular response to IR, at least within the first 48 h after induction of DNA damage.

In light of lack of effect in early responses, we reasoned out the radiosensitivity we observed in 15-days clonogenic assays (Fig 1) could be triggered by a later cellular response. In order to study other biological consequences of IR, we investigated induction of cellular senescence, which is known to onset several days after irradiation [61]. To this end, we assessed IR-induced β-Gal activity 6 days after IR in cells infected with E.V. or shMAPK11, as a well-stablished marker of senescence. As shown in Fig. 4A, A549 cells harbouring shRNA targeting MAPK11 undergo enhanced induction of senescence-like phenotypes compared to E.V. cells. In addition, we confirmed these results by analysing gene expression of well-stablished senescence markers: IL-1β, p21, IL-6 and IL-8 [62], observing a significant induction for all of them after MAPK11 knockdown compared to E.V. cells (Fig. 4B). In sum, our results indicate that the lack of MAPK11 could promote a marked increase in cellular senescence secondary to irradiation.

To verify our observations based on shRNA, we developed a complementary epigenetic perturbation approach based on doxycycline(dox)-inducible CRISPR interference. After achieving an effective knockdown (Fig 5A, Sup 4A), we performed clonogenic assays with A549 cells harbouring a dox-inducible dCas9-KRAB and a non-target control gRNA (NTC) or a gRNA targeting MAPK11 promoter (sgMAPK11). In line with shRNA data, CRISPRi knockdown of MAPK11 was able to sensitize A549 cell line to IR (Fig 5B) showing a lower SF2Gy (NTC=76.05±8.6 ; sgMAPK11=43.65±3.5). Moreover, both biochemical and biological effects of CRISPRi knockdown were similar to those obtained with shRNA: no effect was observed on DNA damage repair, p-ATM foci formation and apoptosis induction (Sup. 4); while, as expected, senescence induction was increased in cells upon MAPK11 CRISPRi knockdown, in terms of both β-Gal staining and expression of senescence-related genes (Fig 5C, D). Collectively, these results confirm those obtained with shRNA interference, and strongly suggests an important role for MAPK11 in mediating the cellular response to IR.

To evaluate the generality of our observation, we assessed β-Gal activity and induction of IL-1β, IL-6, IL-8 and p21 in response to IR in HCT-116 and MCF-7 cell lines with and without MAPK11 expression. In both experimental models, we observed an enhancement of β-Gal activity and gene expression profiler

associated to IR dependent senescence (Fig 6); thus confirming MAPK11 could be involved in the induction of senescence in response to IR. Finally, to evaluate the clinical implications of our findings, we performed an *in silico* analysis by using cBioportal, which stores information from the TCGA database including patient data upon radiotherapy treatment for almost all tumour types. However, the limited number of patients treated with radiotherapy for most tumour types restricted our analyses to breast cancer (643 patients). Interestingly, this in silico analysis points to a clear relationship between MAPK11 expression levels and clinical outcome, in terms of overall survival, of patients undergoing radiotherapy treatment, thus supporting a key role for this MAPK in radiobiology and radiotherapy.

Discussion

IR triggers a broad, complex, and highly regulated cellular response involving a wide variety of signalling pathways and biological processes. Interestingly, we have observed MAPK11 abrogation drives a marked increase in cellular sensitivity to IR, regardless of the gene perturbation approach applied and the cancer cell line studied. To uncover the mechanism leading to this effect, we first investigated the role of MAPK11 in the activity of DDR signalling pathway in early response to IR. Surprisingly, we detected no differences in the cellular response to DNA damage by measuring cell cycle arrest and apoptosis as early responses to IR [63]. Conversely, radiosensitisation associated with MAPK11 knockdown could be explained by a promotion of IR-induced senescence, a critical late-onset cellular effect associated to IR [61] which we confirmed by X-Gal staining and expression of senescence-associated genes. These data establish MAPK11 as a new key player in mediating the array of cellular response to IR, and provide new molecular and biological insights on sensitisation to radiotherapy.

Our study confirms roles previously assigned to p38MAPK in response to IR, since other works have shown p38MAPK is involved in the activation of G2/M and G1/S checkpoints in response to different types of stress [64–66]. Indeed, nuclear translocation of p38MAPK has been observed in response to IR, strongly supporting this signalling pathway should play a role in response to this type of stress [67]. In this sense, p38MAPK may regulate G2/M checkpoint through an indirect gene induction of Gadd45α [68], or more directly by phosphorylating cdc25B [69] and p21 [70], which coordinate cell cycle progression. Given the apparent lack of effect of MAPK11 onto early cell response to IR we observe, it would be interesting to analyse its implication in long term G2/M blockage, a critical process in radiosensitivity [71] whose impaired regulation can lead to senescence induction [72].

The key finding of our work is the observation of a clear MAPK11-dependent enhancement of IR-associated senescence, which may account for the radiosensitivity induced by MAPK11 depletion. A role for p38MAPK signalling pathway in cellular senescence has been previously suggested in response to

different stimuli, for instance after treatment with IR [26], however, this publication employs SB203580 which inhibits both MAPK11 and MAPK14 making impossible to distinguish specific functions. In relation to our data, this signalling pathway has been shown to acutely induce senescence-related cytokines such as IL-6 [73], IL-8 [74], or IL-1β, activated by p38MAPK through C/EBP/NFIL-6 transcription factors [75], which are phosphorylated by MAPK11 in skeletal muscle [76]. p38MAPK have also been identified as a key regulator of oxidative stress-associated senescence in irradiated chondrocytes [77] and fibroblasts undergoing oxidative stress [78]. However additional research is needed to fully clarify the role of MAPK11 in the response to the cell damage induced by ionizing radiation.

Our work clearly demonstrates - for the very first time in radiotherapy - a specific regulatory role for MAPK11, namely in controlling the induction of senescence in response to IR, which seems to be independent of MAPK14. Although there are not many studies that analyse the functions of MAPK11, particularly in radiotherapy, functions related to oxidative stress and senescence have been described for this protein. MAPK11 has been found to protect from oxidative stress-induced cytotoxicity in brain [79], muscle [80] and cardiomyocytes [81]. Interestingly, histone deacetylase HDAC3 interacts directly with MAPK11 supressing its transcription activity [82], and this HDAC has been recently proposed as a key regulator of Senescence Associated Secretory Phenotype (SASP)[83]. However, the molecular mechanisms by which MAPK11 manages the induction of senescence in response to IR remains unexplored.

Conclusions

Our results indicate MAPK11 is a key player in the cellular response to IR trough the control of senescence. This observation suggests MAPK11 to be considered as a potential target for radiosensitisation and/or as a predictive marker for the efficacy of radiotherapy. Nevertheless, further studies are needed to fully clarify the specific mechanisms by which this MAPK triggers IR-associated senescence, and whether our observations extend to other types of cell damage.

Funding

This work has been supported with Grant RTI2018-094093-B-I00/ and PID2021-122222OB-I00 funded by MCIN/AEI/10.13039/501100011033, “ERDF A way of making Europe” to RSP. Also supported with funds from Fundación Leticia Castillejo Castillo, Roche España and ACEPAIN to RSP and MJRH. RSP and MJRH’s Research Institute and the work carried out in their laboratory, received partial support from the European Community through the FEDER. This work was also supported by a European Molecular Biology Organization (EMBO) Short-Term Fellowship to DMFA. JJ holds a predoctoral research contract co-funded by the European Social Fund and UCLM. DV holds a personal Fellowship from the BHF (FS/18/39/33684). ARG and SF are supported by grants from Barts Charity and the BHF (MGU0501 and FS/18/39/33684 to DV).

Conflicts of Interest

The authors declare that they have no known competing financial interests or personal relationships that could have appeared to influence the work reported in this paper.

References

[1] Delaney G, Jacob S, Featherstone C, Barton M. The role of radiotherapy in cancer treatment: estimating optimal utilization from a review of evidence-based clinical guidelines. Cancer 2005;104:1129–37. https://doi.org/10.1002/cncr.21324.

[2] NHS. National Cancer Registration and Analysis Service n.d. https://www.cancerdata.nhs.uk/ (accessed July 18, 2022).

[3] Zhu X, Wang Y, Jiang C, Li X, Sun L, Wang G, et al. Radiosensitivity-Specific Proteomic and Signaling Pathway Network of Non-Small Cell Lung Cancer (NSCLC). International Journal of Radiation Oncology, Biology, Physics 2022;112:529–41. https://doi.org/10.1016/j.ijrobp.2021.08.041.

[4] El-Nachef L, Al-Choboq J, Restier-Verlet J, Granzotto A, Berthel E, Sonzogni L, et al. Human Radiosensitivity and Radiosusceptibility: What Are the Differences? Int J Mol Sci 2021;22:7158. https://doi.org/10.3390/ijms22137158.

[5] de Mey S, Dufait I, De Ridder M. Radioresistance of Human Cancers: Clinical Implications of Genetic Expression Signatures. Frontiers in Oncology 2021;11.

[6] Fowler JF. Chemical modifiers of radiosensitivity-theory and reality: A review. International Journal of Radiation Oncology, Biology, Physics 1985;11:665–74. https://doi.org/10.1016/0360-3016(85)90296-2.

[7] Park HS, You GE, Yang KH, Kim JY, An S, Song J-Y, et al. Role of AKT and ERK pathways in controlling sensitivity to ionizing radiation and adaptive response induced by low-dose radiation in human immune cells. Eur J Cell Biol 2015;94:653–60. https://doi.org/10.1016/j.ejcb.2015.08.003.

[8] Zhou S, Zhang M, Zhou C, Wang W, Yang H, Ye W. The role of epithelial-mesenchymal transition in regulating radioresistance. Critical Reviews in Oncology/Hematology 2020;150:102961. https://doi.org/10.1016/j.critrevonc.2020.102961.

[9] Pawlik TM, Keyomarsi K. Role of cell cycle in mediating sensitivity to radiotherapy. Int J Radiat Oncol Biol Phys 2004;59:928–42. https://doi.org/10.1016/j.ijrobp.2004.03.005.

[10] Vallard A, Bernichon E, Wang Q, Attignon V, Pissaloux D, Bachelot T, et al. Genomic Alterations and Radioresistance in Breast Cancer: An Analysis of the Profiler Protocol. International Journal of Radiation Oncology, Biology, Physics 2017;99:S52. https://doi.org/10.1016/j.ijrobp.2017.06.132.

[11] Rowinski E, Magné N, Fayette J, Daguenet E, Racadot S, Pommier P, et al. Radioresistance and genomic alterations in head and neck squamous cell cancer: Sub-analysis of the ProfiLER protocol. Head Neck 2021;43:3899–910. https://doi.org/10.1002/hed.26891.

[12] Belli M, Tabocchini MA. Ionizing Radiation-Induced Epigenetic Modifications and Their Relevance to Radiation Protection. International Journal of Molecular Sciences 2020;21:5993. https://doi.org/10.3390/ijms21175993.

[13] Suzuki K, Kodama S, Watanabe M. Extremely Low-Dose Ionizing Radiation Causes Activation of Mitogen-activated Protein Kinase Pathway and Enhances Proliferation of Normal Human Diploid Cells. Cancer Res 2001;61:5396–401.

[14] Wang T, Carraway RE, LaRoche D, FitzGerald TJ. Disruption of ERK1/2 Sensitizes Radiation Resistance Prostate Cancer Cells to Paclitaxel and Ionizing Radiation. International Journal of Radiation Oncology, Biology, Physics 2014;90:S806. https://doi.org/10.1016/j.ijrobp.2014.05.2326.

[15] Lee SA, Dritschilo A, Jung M. Impaired Ionizing Radiation-induced Activation of a Nuclear Signal Essential for Phosphorylation of c-Jun by Dually Phosphorylated c-Jun Amino-terminal Kinases in Ataxia Telangiectasia Fibroblasts *. Journal of Biological Chemistry 1998;273:32889–94. https://doi.org/10.1074/jbc.273.49.32889.

[16] Hamdi M, Kool J, Cornelissen-Steijger P, Carlotti F, Popeijus HE, van der Burgt C, et al. DNA damage in transcribed genes induces apoptosis via the JNK pathway and the JNK-phosphatase MKP-1. Oncogene 2005;24:7135–44. https://doi.org/10.1038/sj.onc.1208875.

[17] Rosette C, Karin M. Ultraviolet light and osmotic stress: activation of the JNK cascade through multiple growth factor and cytokine receptors. Science 1996;274:1194–7. https://doi.org/10.1126/science.274.5290.1194.

[18] Ruvolo PP. Intracellular signal transduction pathways activated by ceramide and its metabolites. Pharmacol Res 2003;47:383–92. https://doi.org/10.1016/s1043-6618(03)00050-1.

[19] Van Meter M, Simon M, Tombline G, May A, Morello TD, Hubbard BP, et al. JNK Phosphorylates SIRT6 to Stimulate DNA Double-Strand Break Repair in Response to Oxidative Stress by Recruiting PARP1 to DNA Breaks. Cell Rep 2016;16:2641–50. https://doi.org/10.1016/j.celrep.2016.08.006.

[20] Angulo-Ibáñez M, Rovira-Clavé X, Espel E. ATM meets ERK5. Aging (Albany NY) 2017;9:299–300. https://doi.org/10.18632/aging.101189.

[21] Broustas CG, Duval AJ, Chaudhary KR, Friedman RA, Virk RK, Lieberman HB. Targeting MEK5 impairs nonhomologous end-joining repair and sensitizes prostate cancer to DNA damaging agents. Oncogene 2020;39:2467–77. https://doi.org/10.1038/s41388-020-1163-1.

[22] Jinlian L, Yingbin Z, Chunbo W. p38 MAPK in regulating cellular responses to ultraviolet radiation. J Biomed Sci 2007;14:303–12. https://doi.org/10.1007/s11373-007-9148-4.

[23] Lee JC, Laydon JT, McDonnell PC, Gallagher TF, Kumar S, Green D, et al. A protein kinase involved in the regulation of inflammatory cytokine biosynthesis. Nature 1994;372:739–46. https://doi.org/10.1038/372739a0.

[24] Cho JH, Hong WG, Jung Y-J, Lee J, Lee E, Hwang S-G, et al. Γ-Ionizing radiation-induced activation of the EGFR-p38/ERK-STAT3/CREB-1-EMT pathway promotes the migration/invasion of non-small cell lung cancer cells and is inhibited by podophyllotoxin acetate. Tumour Biol 2016;37:7315–25. https://doi.org/10.1007/s13277-015-4548-y.

[25] Wang X, McGowan CH, Zhao M, He L, Downey JS, Fearns C, et al. Involvement of the MKK6-p38γ Cascade in γ-Radiation-Induced Cell Cycle Arrest. Mol Cell Biol 2000;20:4543–52.

[26] Wang Y, Liu L, Zhou D. Inhibition of p38 MAPK attenuates ionizing radiation-induced hematopoietic cell senescence and residual bone marrow injury. Radiat Res 2011;176:743–52. https://doi.org/10.1667/rr2727.1.

[27] Cuenda A, Rousseau S. p38 MAP-Kinases pathway regulation, function and role in human diseases. Biochimica et Biophysica Acta (BBA) - Molecular Cell Research 2007;1773:1358–75. https://doi.org/10.1016/j.bbamcr.2007.03.010.

[28] Korb A, Tohidast-Akrad M, Cetin E, Axmann R, Smolen J, Schett G. Differential tissue expression and activation of p38 MAPK alpha, beta, gamma, and delta isoforms in rheumatoid arthritis. Arthritis Rheum 2006;54:2745–56. https://doi.org/10.1002/art.22080.

[29] Yang C, Cao P, Gao Y, Wu M, Lin Y, Tian Y, et al. Differential expression of p38 MAPK α, β, γ, δ isoforms in nucleus pulposus modulates macrophage polarization in intervertebral disc degeneration. Sci Rep 2016;6:22182. https://doi.org/10.1038/srep22182.

[30] Wang H, Xu Q, Xiao F, Jiang Y, Wu Z. Involvement of the p38 Mitogen-activated Protein Kinase α, β, and γ Isoforms in Myogenic Differentiation. MBoC 2008;19:1519–28. https://doi.org/10.1091/mbc.e07-08-0817.

[31] Katopodis P, Kerslake R, Zikopoulos A, Beri N, Anikin V. p38β - MAPK11 and its role in female cancers. Journal of Ovarian Research 2021;14:84. https://doi.org/10.1186/s13048-021-00834-9.

[32] Qin J-Z, Xin H, Qi X-M, Chen G. Isoform-specific and cell/tissue-dependent effects of p38 MAPKs in regulating inflammation and inflammation-associated oncogenesis. Frontiers in Bioscience-Landmark 2022;27:31. https://doi.org/10.31083/j.fbl2701031.

[33] García-Cano J, Roche O, Cimas FJ, Pascual-Serra R, Ortega-Muelas M, Fernández-Aroca DM, et al. p38MAPK and Chemotherapy: We Always Need to Hear Both Sides of the Story. Front Cell Dev Biol 2016;4:69. https://doi.org/10.3389/fcell.2016.00069.

[34] Pramanik R, Qi X, Borowicz S, Choubey D, Schultz RM, Han J, et al. p38 Isoforms Have Opposite Effects on AP-1-dependent Transcription through Regulation of c-Jun: THE DETERMINANT ROLE OF THE ISOFORMS IN THE p38 MAPK SIGNAL SPECIFICITY*. Journal of Biological Chemistry 2003;278:4831–9. https://doi.org/10.1074/jbc.M207732200.

[35] Canovas B, Nebreda AR. Diversity and versatility of p38 kinase signalling in health and disease. Nat Rev Mol Cell Biol 2021;22:346–66. https://doi.org/10.1038/s41580-020-00322-w.

[36] Del Reino P, Alsina-Beauchamp D, Escós A, Cerezo-Guisado MI, Risco A, Aparicio N, et al. Pro-oncogenic role of alternative p38 mitogen-activated protein kinases p38γ and p38δ, linking inflammation and cancer in colitis-associated colon cancer. Cancer Res 2014;74:6150–60. https://doi.org/10.1158/0008-5472.CAN-14-0870.

[37] Fajardo P, Taskova M, Martín-Serrano MA, Hansen J, Slott S, Jakobsen AK, et al. p38γ and p38δ as biomarkers in the interplay of colon cancer and inflammatory bowel diseases. Cancer Commun (Lond) 2022. https://doi.org/10.1002/cac2.12331.

[38] Roche O, Fernández-Aroca DM, Arconada-Luque E, García-Flores N, Mellor LF, Ruiz-Hidalgo MJ, et al. p38β and Cancer: The Beginning of the Road. Int J Mol Sci 2020;21:E7524. https://doi.org/10.3390/ijms21207524.

[39] Raman M, Earnest S, Zhang K, Zhao Y, Cobb MH. TAO kinases mediate activation of p38 in response to DNA damage. EMBO J 2007;26:2005–14. https://doi.org/10.1038/sj.emboj.7601668.

[40] Im J-S, Lee J-K. ATR-dependent Activation of p38 MAP Kinase Is Responsible for Apoptotic Cell Death in Cells Depleted of Cdc7 *. Journal of Biological Chemistry 2008;283:25171–7. https://doi.org/10.1074/jbc.M802851200.

[41] Choi S-Y, Kim M-J, Kang C-M, Bae S, Cho C-K, Soh J-W, et al. Activation of Bak and Bax through c-Abl-Protein Kinase Cδ-p38 MAPK Signaling in Response to Ionizing Radiation in Human Non-small Cell Lung Cancer Cells *. Journal of Biological Chemistry 2006;281:7049–59. https://doi.org/10.1074/jbc.M512000200.

[42] Kim M-J, Byun J-Y, Yun C-H, Park I-C, Lee K-H, Lee S-J. c-Src-p38 mitogen-activated protein kinase signaling is required for Akt activation in response to ionizing radiation. Mol Cancer Res 2008;6:1872–80. https://doi.org/10.1158/1541-7786.MCR-08-0084.

[43] Pascual-Serra R, Fernández-Aroca DM, Sabater S, Roche O, Andrés I, Ortega-Muelas M, et al. p38β (MAPK11) mediates gemcitabine-associated radiosensitivity in sarcoma experimental models. Radiother Oncol 2021;156:136–44. https://doi.org/10.1016/j.radonc.2020.12.008.

[44] Fulco CP, Munschauer M, Anyoha R, Munson G, Grossman SR, Perez EM, et al. Systematic mapping of functional enhancer-promoter connections with CRISPR interference. Science 2016;354:769–73. https://doi.org/10.1126/science.aag2445.

[45] Gilbert LA, Horlbeck MA, Adamson B, Villalta JE, Chen Y, Whitehead EH, et al. Genome-Scale CRISPR-Mediated Control of Gene Repression and Activation. Cell 2014;159:647–61. https://doi.org/10.1016/j.cell.2014.09.029.

[46] Serrano-Oviedo L, Ortega-Muelas M, García-Cano J, Valero ML, Cimas FJ, Pascual-Serra R, et al. Autophagic cell death associated to Sorafenib in renal cell carcinoma is mediated through Akt inhibition in an ERK1/2 independent fashion. PLoS ONE 2018;13:e0200878. https://doi.org/10.1371/journal.pone.0200878.

[47] Cimas FJ, Callejas-Valera JL, García-Olmo DC, Hernández-Losa J, Melgar-Rojas P, Ruiz-Hidalgo MJ, et al. E1a is an exogenous in vivo tumour suppressor. Cancer Lett 2017;399:74–81. https://doi.org/10.1016/j.canlet.2017.04.010.

[48] Mandegar MA, Huebsch N, Frolov EB, Shin E, Truong A, Olvera MP, et al. CRISPR Interference Efficiently Induces Specific and Reversible Gene Silencing in Human iPSCs. Cell Stem Cell 2016;18:541–53. https://doi.org/10.1016/j.stem.2016.01.022.

[49] Labun K, Montague TG, Krause M, Torres Cleuren YN, Tjeldnes H, Valen E. CHOPCHOP v3: expanding the CRISPR web toolbox beyond genome editing. Nucleic Acids Research 2019;47:W171–4. https://doi.org/10.1093/nar/gkz365.

[50] Stojic L. Tuning the Expression of Long Noncoding RNA Loci with CRISPR Interference. Methods Mol Biol 2020;2161:1–16. https://doi.org/10.1007/978-1-0716-0680-3_1.

[51] Valero ML, Cimas FJ, Arias L, Melgar-Rojas P, García E, Callejas-Valera JL, et al. E1a promotes c-Myc-dependent replicative stress: implications in glioblastoma radiosensitization. Cell Cycle 2014;13:52–61. https://doi.org/10.4161/cc.26754.

[52] González JE, Lee M, Barquinero JF, Valente M, Roch-Lefèvre S, García O. Quantitative image analysis of gamma-H2AX foci induced by ionizing radiation applying open source programs. Anal Quant Cytol Histol 2012;34:66–71.

[53] de la Cruz-Morcillo MA, García-Cano J, Arias-González L, García-Gil E, Artacho-Cordón F, Ríos-Arrabal S, et al. Abrogation of the p38 MAPK α signaling pathway does not promote radioresistance but its activity is required for 5-Fluorouracil-associated radiosensitivity. Cancer Lett 2013;335:66–74. https://doi.org/10.1016/j.canlet.2013.01.050.

[54] Franken NAP, Rodermond HM, Stap J, Haveman J, van Bree C. Clonogenic assay of cells in vitro. Nat Protoc 2006;1:2315–9. https://doi.org/10.1038/nprot.2006.339.

[55] van Leeuwen CM, Oei AL, Crezee J, Bel A, Franken N a. P, Stalpers LJA, et al. The alfa and beta of tumours: a review of parameters of the linear-quadratic model, derived from clinical radiotherapy studies. Radiat Oncol 2018;13:96. https://doi.org/10.1186/s13014-018-1040-z.

[56] Adrados I, Larrasa-Alonso J, Galarreta A, López-Antona I, Menéndez C, Abad M, et al. The homeoprotein SIX1 controls cellular senescence through the regulation of p16INK4A and differentiation-related genes. Oncogene 2016;35:3485–94. https://doi.org/10.1038/onc.2015.408.

[57] Fernández-Aroca DM, Roche O, Sabater S, Pascual-Serra R, Ortega-Muelas M, Sánchez Pérez I, et al. P53 pathway is a major determinant in the radiosensitizing effect of Palbociclib: Implication in cancer therapy. Cancer Letters 2019;451:23–33. https://doi.org/10.1016/j.canlet.2019.02.049.

[58] Olive PL, Banáth JP. The comet assay: a method to measure DNA damage in individual cells. Nat Protoc 2006;1:23–9. https://doi.org/10.1038/nprot.2006.5.

[59] Gyori BM, Venkatachalam G, Thiagarajan PS, Hsu D, Clement M-V. OpenComet: An automated tool for comet assay image analysis. Redox Biology 2014;2:457–65. https://doi.org/10.1016/j.redox.2013.12.020.

[60] Gao J, Aksoy BA, Dogrusoz U, Dresdner G, Gross B, Sumer SO, et al. Integrative Analysis of Complex Cancer Genomics and Clinical Profiles Using the cBioPortal. Sci Signal 2013;6:pl1. https://doi.org/10.1126/scisignal.2004088.

[61] Luo H, Yount C, Lang H, Yang A, Riemer EC, Lyons K, et al. Activation of p53 with Nutlin-3a radiosensitizes lung cancer cells via enhancing radiation-induced premature senescence. Lung Cancer 2013;81:167–73. https://doi.org/10.1016/j.lungcan.2013.04.017.

[62] López-Antona I, Contreras-Jurado C, Luque-Martín L, Carpintero-Leyva A, González-Méndez P, Palmero I. Dynamic regulation of myofibroblast phenotype in cellular senescence. Aging Cell 2022;21:e13580. https://doi.org/10.1111/acel.13580.

[63] Little JB. Principal Cellular and Tissue Effects of Radiation. Holland-Frei Cancer Medicine 6th Edition 2003.

[64] Mikhailov A, Shinohara M, Rieder CL. Topoisomerase II and histone deacetylase inhibitors delay the G2/M transition by triggering the p38 MAPK checkpoint pathway. J Cell Biol 2004;166:517–26. https://doi.org/10.1083/jcb.200405167.

[65] Bulavin DV, Amundson SA, Fornace AJ. p38 and Chk1 kinases: different conductors for the G(2)/M checkpoint symphony. Curr Opin Genet Dev 2002;12:92–7. https://doi.org/10.1016/s0959-437x(01)00270-2.

[66] Dmitrieva NI, Bulavin DV, Fornace AJ, Burg MB. Rapid activation of G2/M checkpoint after hypertonic stress in renal inner medullary epithelial (IME) cells is protective and requires p38 kinase. Proceedings of the National Academy of Sciences 2002;99:184–9. https://doi.org/10.1073/pnas.231623498.

[67] Wood CD, Thornton TM, Sabio G, Davis RA, Rincon M. Nuclear localization of p38 MAPK in response to DNA damage. Int J Biol Sci 2009;5:428–37. https://doi.org/10.7150/ijbs.5.428.

[68] Zhu N, Shao Y, Xu L, Yu L, Sun L. Gadd45-α and Gadd45-γ utilize p38 and JNK signaling pathways to induce cell cycle G2/M arrest in Hep-G2 hepatoma cells. Mol Biol Rep 2008;36:2075. https://doi.org/10.1007/s11033-008-9419-9.

[69] Thornton TM, Rincon M. Non-Classical P38 Map Kinase Functions: Cell Cycle Checkpoints and Survival. Int J Biol Sci 2008;5:44–52.

[70] Kim G-Y, Mercer SE, Ewton DZ, Yan Z, Jin K, Friedman E. The stress-activated protein kinases p38 alpha and JNK1 stabilize p21(Cip1) by phosphorylation. J Biol Chem 2002;277:29792–802. https://doi.org/10.1074/jbc.M201299200.

[71] Liu C, Nie J, Wang R, Mao W. The Cell Cycle G2/M Block Is an Indicator of Cellular Radiosensitivity. Dose Response 2019;17:1559325819891008. https://doi.org/10.1177/1559325819891008.

[72] Roger L, Tomas F, Gire V. Mechanisms and Regulation of Cellular Senescence. Int J Mol Sci 2021;22:13173. https://doi.org/10.3390/ijms222313173.

[73] Ono K, Han J. The p38 signal transduction pathway: activation and function. Cell Signal 2000;12:1–13. https://doi.org/10.1016/s0898-6568(99)00071-6.

[74] Song Y-H, Chai Q, Wang N, Yang F-F, Wang G-H, Hu J-Y. X-rays induced IL-8 production in lung cancer cells via p38/MAPK and NF-κB pathway. Int J Radiat Biol 2020;96:1374–81. https://doi.org/10.1080/09553002.2020.1683643.

[75] Baldassare JJ, Bi Y, Bellone CJ. The Role of p38 Mitogen-Activated Protein Kinase in IL-1β Transcription. The Journal of Immunology 1999;162:5367–73.

[76] Zhang G, Li Y-P. p38β MAPK upregulates atrogin1/MAFbx by specific phosphorylation of C/EBPβ. Skeletal Muscle 2012;2:20. https://doi.org/10.1186/2044-5040-2-20.

[77] Hong E-H, Lee S-J, Kim J-S, Lee K-H, Um H-D, Kim J-H, et al. Ionizing Radiation Induces Cellular Senescence of Articular Chondrocytes via Negative Regulation of SIRT1 by p38 Kinase*. Journal of Biological Chemistry 2010;285:1283–95. https://doi.org/10.1074/jbc.M109.058628.

[78] Dasari A, Bartholomew JN, Volonte D, Galbiati F. Oxidative Stress Induces Premature Senescence by Stimulating Caveolin-1 Gene Transcription through p38 Mitogen-Activated Protein Kinase/Sp1–Mediated Activation of Two GC-Rich Promoter Elements. Cancer Research 2006;66:10805–14. https://doi.org/10.1158/0008-5472.CAN-06-1236.

[79] Shin J-H, Jeong J-Y, Jin Y, Kim I-D, Lee J-K. p38β MAPK affords cytoprotection against oxidative stress-induced astrocyte apoptosis via induction of αB-crystallin and its anti-apoptotic function. Neurosci Lett 2011;501:132–7. https://doi.org/10.1016/j.neulet.2011.06.061.

[80] McClung JM, Judge AR, Powers SK, Yan Z. p38 MAPK links oxidative stress to autophagy-related gene expression in cachectic muscle wasting. Am J Physiol Cell Physiol 2010;298:C542–9. https://doi.org/10.1152/ajpcell.00192.2009.

[81] Kim JK, Pedram A, Razandi M, Levin ER. Estrogen prevents cardiomyocyte apoptosis through inhibition of reactive oxygen species and differential regulation of p38 kinase isoforms. J Biol Chem 2006;281:6760–7. https://doi.org/10.1074/jbc.M511024200.

[82] Mahlknecht U, Will J, Varin A, Hoelzer D, Herbein G. Histone Deacetylase 3, a Class I Histone Deacetylase, Suppresses MAPK11-Mediated Activating Transcription Factor-2 Activation and Represses TNF Gene Expression. The Journal of Immunology 2004;173:3979–90. https://doi.org/10.4049/jimmunol.173.6.3979.

[83] Eichner LJ, Curtis SD, Brun SN, Baumgart JT, Ross DS, Rymoff TJ, et al. HDAC3 regulates senescence and lineage specificity in non-small cell lung cancer 2021:2020.10.14.338590. https://doi.org/10.1101/2020.10.14.338590.

Figure Legend

Fig. 1. Genetic abrogation of MAPK11 promotes radiosensitivity in A549, HCT-116 and MCF-7 cell lines.
A) A549 cells were infected with lentiviruses carrying empty vector (E.V), shRNA for MAPK11 (shMAPK11) or MAPK14 (shMAPK14). Genetic interference was evaluated by western blot using tubulin as a loading control. Bars denote standard deviation (S.D).
B) Clonogenic assays for A549 cells infected with E.V, shMAPK11 or shMAPK14 and exposed to the indicated doses of X rays. Surviving fraction was normalized to respective unirradiated controls. Bars mean standard deviation (S.D).
C) A549 E.V., shMAPK11 and shMAPK14 surviving fraction at 2 Gy (SF2Gy) ± S.D. calculated by lineal-quadratic model.
D) Same as in A) for HCT-116 cells. E) Same as in B) for HCT-116 cells. F) Same as in C) for HCT-116 cells. G) Same as in A) for MCF-7 cells. H) Same as in B) for MCF-7 cells. I) Same as in C) for MCF-7 cells.

Fig. 2. MAPK11 does not modulate DDR activity and DNA repair in response to ionising radiation.
A) *Upper panel*: A549 cells harbouring empty vector (E.V.) or shMAPK11 were plated onto cell culture slides 24 h prior to irradiation (10 Gy) and 4 h later cells were fixed and processed for immunocytochemistry against phospho-ATM (Ser1981) or phospho-BRCA1 (Ser1524). Images show a representative cell out of a minimum of 100 analysed. *Lower panel*: Quantification of phospho-ATM or phospho-BRCA1 foci number per nuclei in three independent experiments. Bars mean standard deviation (S.D).
B) *Left panel*: Comet assay analysis of A549 E.V. and shMAPK11 cells. After irradiation (10Gy) DNA damage was evaluated at the indicated times. Images show a representative cell out of a minimum of 100 analysed. *Right panel*: Histogram showing comet tail moment normalized to E.V. unirradiated controls. Bars mean standard deviation (S.D).

Fig. 3. MAPK11 does not deregulate cell cycle and apoptosis after irradiation in A549 cell line.
A) *Upper panel*: Image of a representative cell cycle profile in A549 E.V. and shMAPK11 cells irradiated at 10 Gy. Cell cycle was evaluated by flow cytometry at indicated times after IR. *Lower panel*: Histogram showing the average of three independent experiments representing the percentage of population in the different phases of the cell cycle. Bars mean S.D.
B) *Upper panel*: Graphical representation of apoptosis induction in A549 E.V. and shMAPK11 cells 48 h after irradiation (10 Gy) by staining with Annexin V-FITC/Propidium Iodide for assay by flow cytometry. *Lower panel*: Histogram showing the average of three independent experiments to evaluate the percentage of apoptotic A549 E.V. or shMAPK11 cells 48 h after IR (10 Gy). Bars mean S.D.

Fig. 4. MAPK11 genetic interference enhances cell senescence in response to ionizing radiation.
A) Upper panel: A549 E.V. or shMAPK11 cells were irradiated (10 Gy) and 5 days later β-Gal activity was detected by X-gal staining. A representative image is shown. Scale bars represent 10 μm. Lower panel: Histogram showing the average of, at least, three independent experiments representing the percentage of positive senescent cells. Bars mean S.D.
B) Gene expression of indicated senescence-associated genes was evaluated 5 days after IR (10 Gy) in A549 E.V. or shMAPK11 cells by RT-qPCR using GAPDH as endogenous control. Data were referred to unirradiated E.V. cells. Bars mean S.D.

Fig. 5. Epigenetic perturbation of MAPK11 by CRISPRi confirms its role in cell response to ionizing radiation.

A) A549 cells expressing dCas9 were infected with lentiviruses carrying non-target-control (NTC) or MAPK11-targeted sgRNAs (sgMAPK11). Interference was evaluated by RT-qPCR using GAPDH as an endogenous control (right) and by western blot using tubulin as a loading control (left). Bars mean standard deviation (S.D).

B) Clonogenic assays for A549 NTC and sgMAPK11 cell exposed to the indicated doses of X rays. Bars mean standard deviation (S.D).

C) Histograms show the average of three independent experiments representing the percentage of positive senescent cells evaluated by X-Gal staining 5 days after IR (10 Gy). Bars indicate S.D.

D) Gene expression of indicated senescence-associated genes was evaluated 5 days after IR (10 Gy) in A549 NTC or sgMAPK11 cells by RT-qPCR using GAPDH as endogenous control. Data were referred to unirradiated NTC cells. Bars mean S.D.

Figure 6. Genetic interference of MAPK11 increases induction of senescence in response to ionizing radiation in HCT-116 and MCF-7 cell lines.

A) HCT-116 E.V. and shMAPK11 cells were irradiated (10 Gy) and 5 days later senescence was evaluated by X-Gal staining. Histogram shows the average of three independent experiments representing the percentage of positive senescent cells. Bars mean S.D.

B) Gene expression of indicated senescence-associated genes was evaluated 5 days after IR (10 Gy) in HCT-116 E.V. and shMAPK11 cells by RT-qPCR using GAPDH as endogenous control. Data were referred to unirradiated E.V. cells. Bars mean S.D.

C) Same as in A) for MCF-7 cells. D) Same as in B) for MCF-7 cells. E) Kaplan–Meyer comparing prognosis in terms of Overall Survival (OS) for two groups of patients, those with high (mRNA expression > 1.2 S.D., n=57) and low (mRNA expression < 1.2 S.D., n=491) expression levels of MAPK11 for IR-treated breast patients from TCGA dataset.

Fig. 1

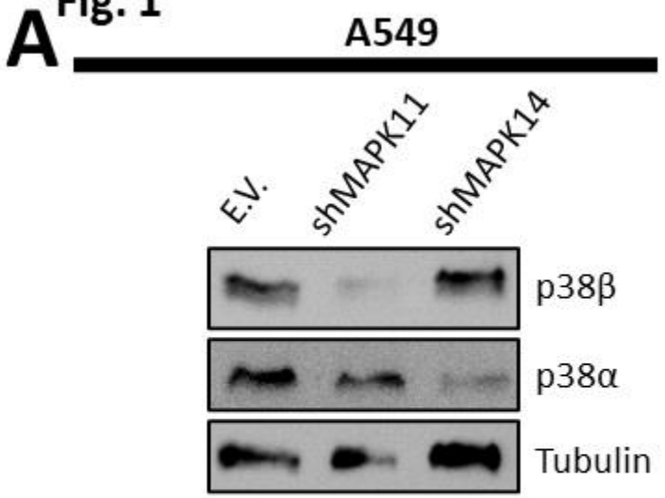

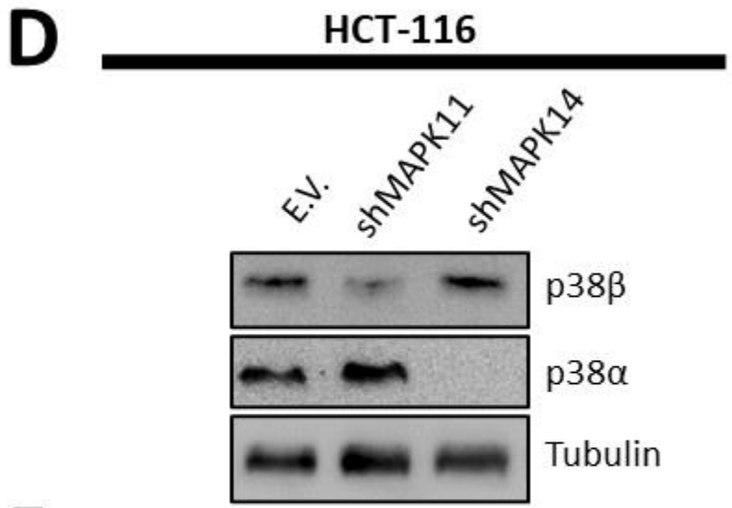

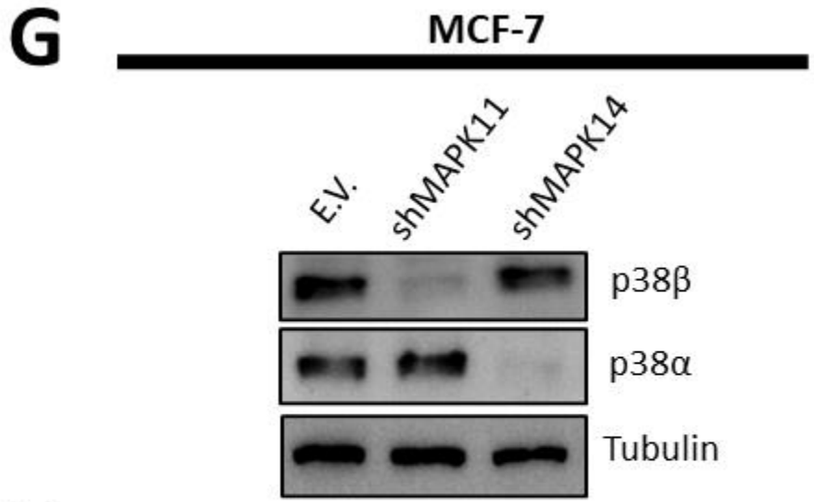

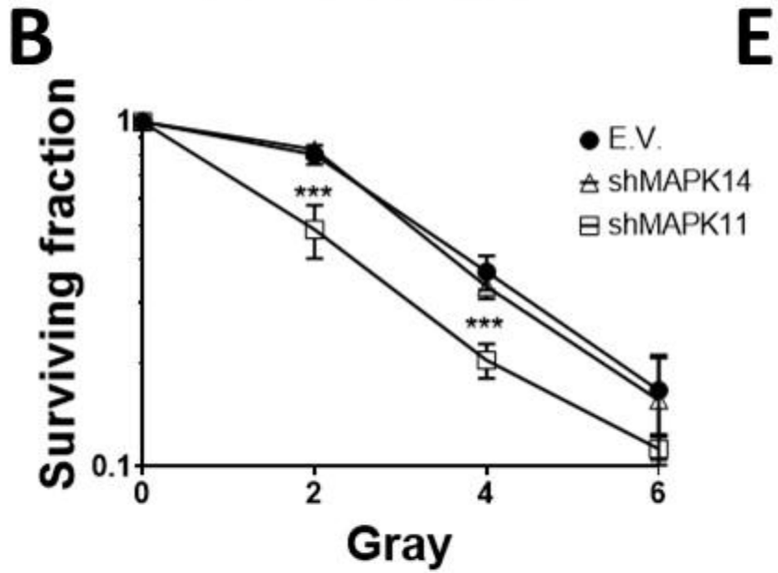

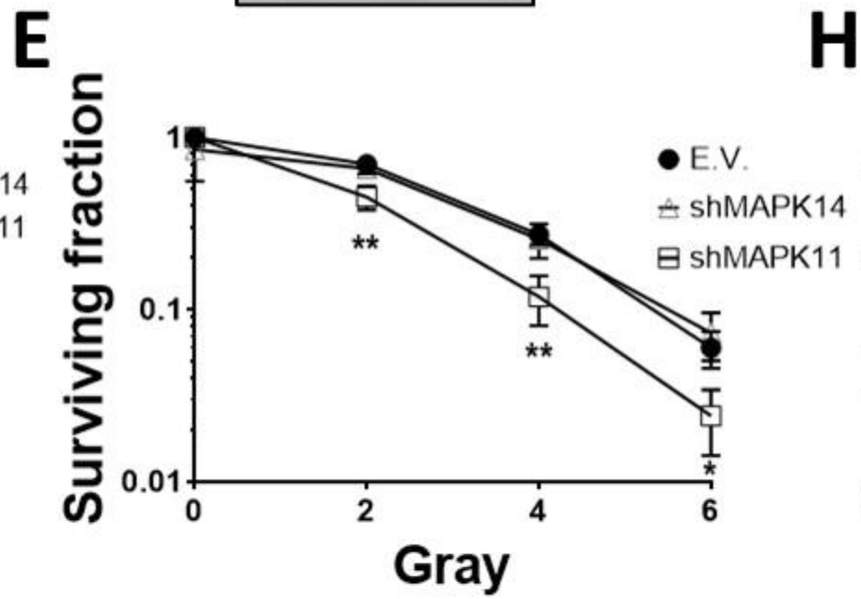

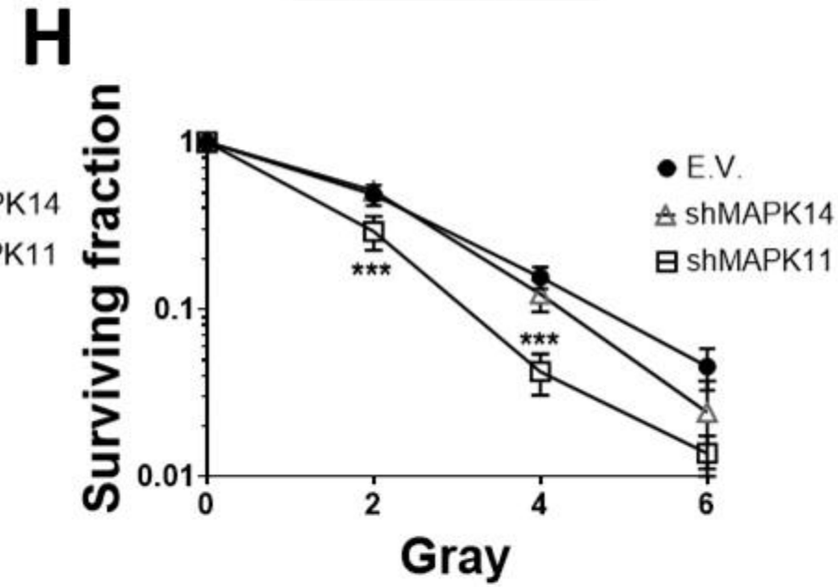

C

Cell line	SF2Gy
A549 E.V.	78,69 ± 5,1
A549 shMAPK11	47,92 ± 7,6
A549 shMAPK14	69,91 ± 4,3

F

Cell line	SF2Gy
HCT116 E.V.	69,97 ± 7,4
HCT116 shMAPK11	44,97 ± 7,1
HCT116 shMAPK14	65,60 ± 6,3

I

Cell line	SF2Gy
MCF-7 E.V.	53,91 ± 6,7
MCF-7 shMAPK11	31,79 ± 4,9
MCF-7 shMAPK14	51,04 ± 5,5

Fig. 2

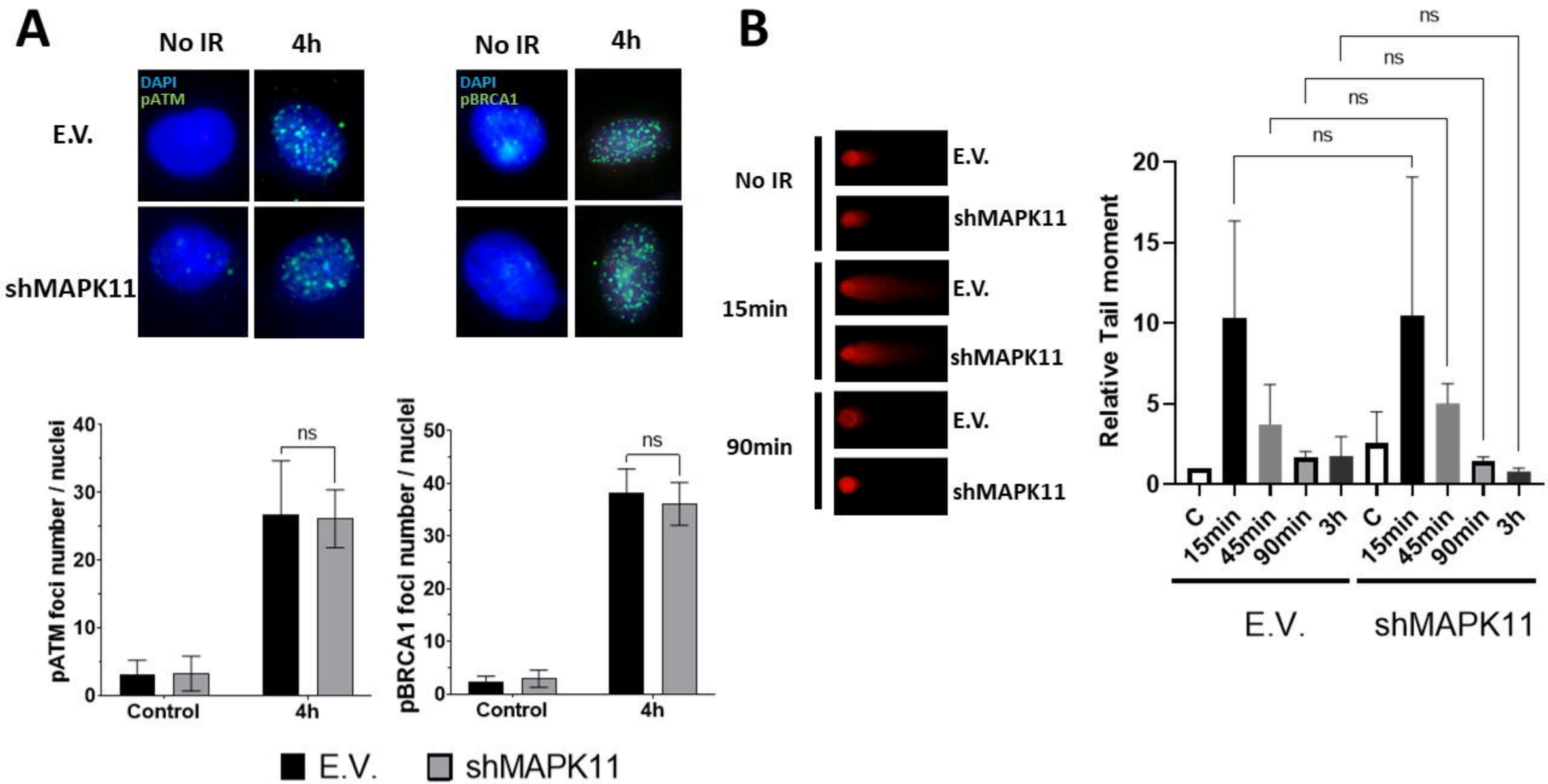
A
No IR
4h
No IR
4h
DAPI
pATM
DAPI
pBRCA1
E.V.
shMAPK11
pATM foci number / nuclei
pBRCA1 foci number / nuclei
ns
Control
4h
E.V.
shMAPK11
B
No IR
15min
90min
E.V.
shMAPK11
Relative Tail moment
ns
C
15min
45min
90min
3h
E.V.
shMAPK11

Fig. 3

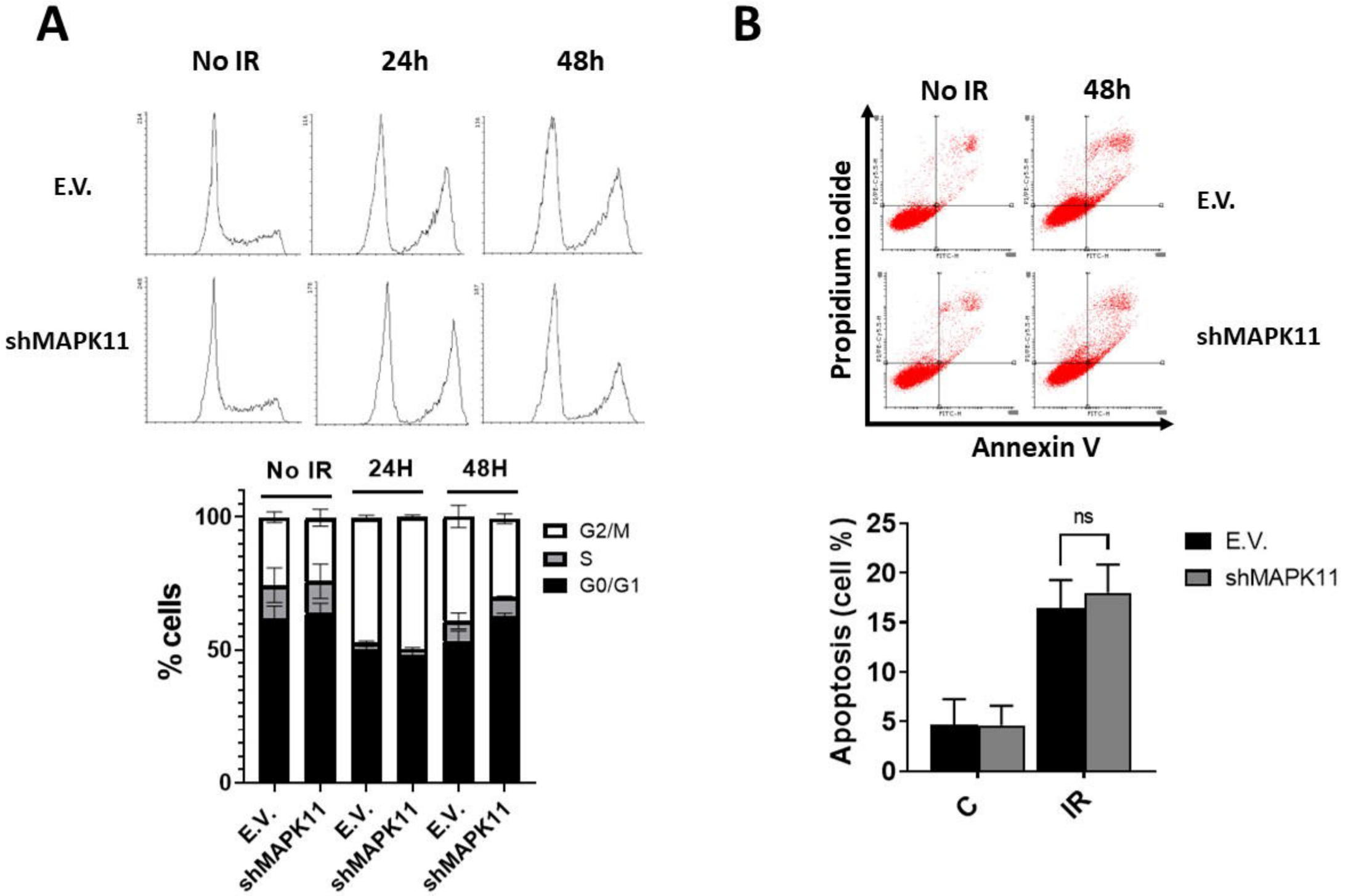
A
No IR
24h
48h
E.V.
shMAPK11
No IR
24H
48H
% cells
100
50
0
G2/M
S
G0/G1
E.V.
shMAPK11
E.V.
shMAPK11
E.V.
shMAPK11
B
No IR
48h
Propidium iodide
Annexin V
E.V.
shMAPK11
Apoptosis (cell %)
25
20
15
10
5
0
ns
E.V.
shMAPK11
C
IR

Fig. 4

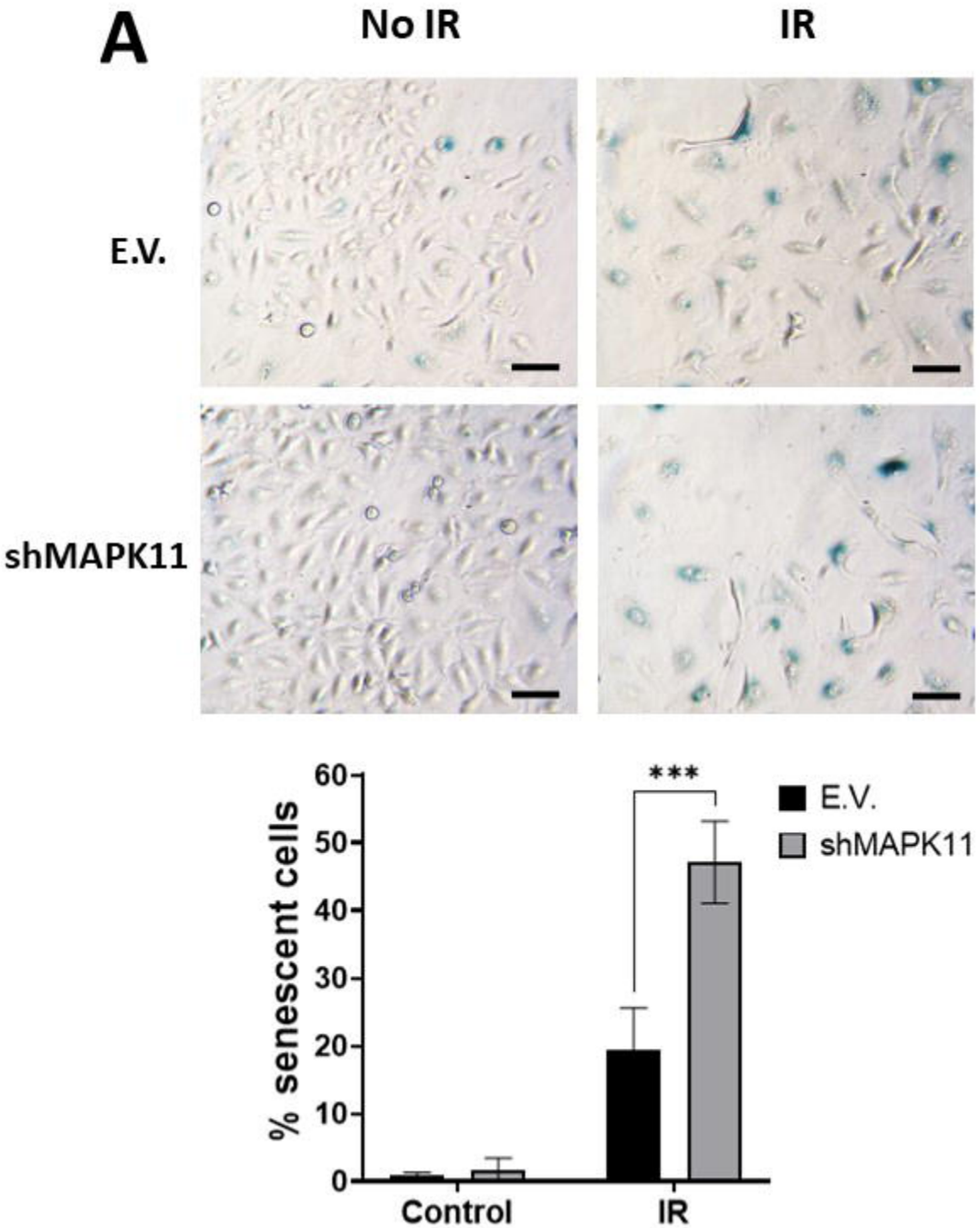
A
No IR
IR
E.V.
shMAPK11
% senescent cells
60
50
40
30
20
10
0
***
E.V.
shMAPK11
Control
IR

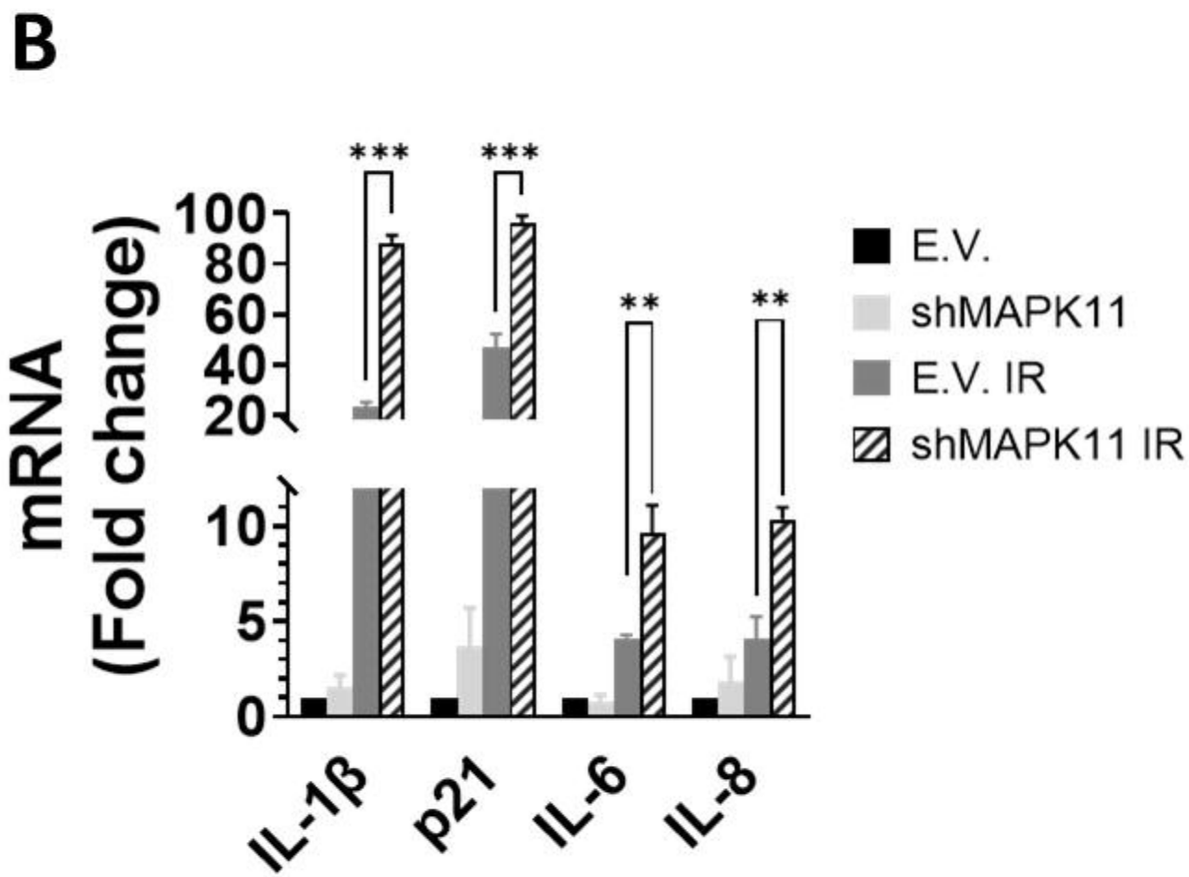
B
mRNA
(Fold change)
100
80
60
40
20
10
5
0
***
***
**
**
E.V.
shMAPK11
E.V. IR
shMAPK11 IR
IL-1β
p21
IL-6
IL-8

Fig. 5

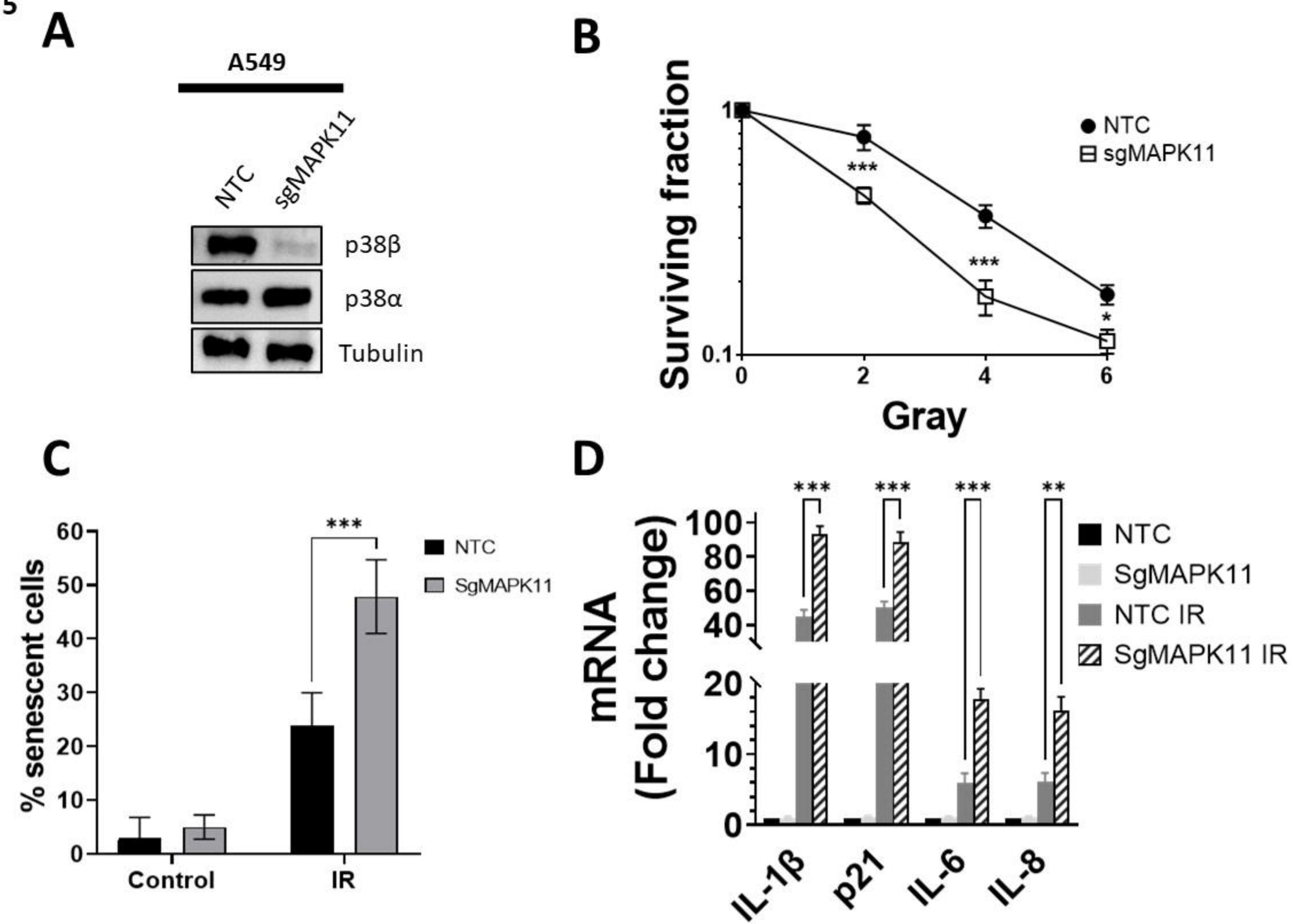
A
A549
NTC
sgMAPK11
p38β
p38α
Tubulin
B
Surviving fraction
1
0.1
0
2
4
6
Gray
NTC
sgMAPK11
***
***
*
C
% senescent cells
60
50
40
30
20
10
0
***
NTC
SgMAPK11
Control
IR
D
mRNA
(Fold change)
100
80
60
40
20
10
0
***
***
***
**
NTC
SgMAPK11
NTC IR
SgMAPK11 IR
IL-1β
p21
IL-6
IL-8

Fig. 6

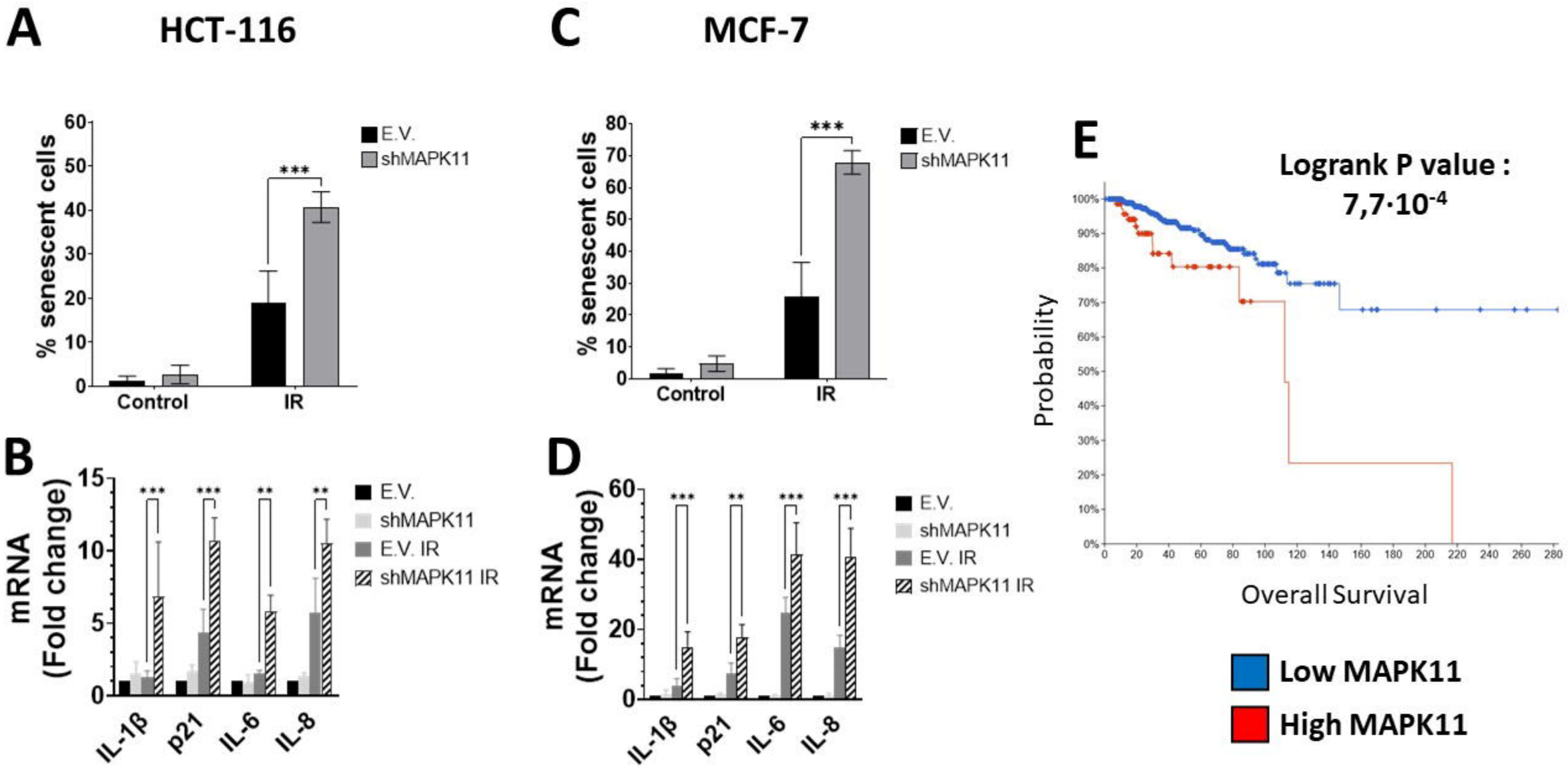
A
HCT-116
% senescent cells
E.V.
shMAPK11
***
Control
IR
B
mRNA (Fold change)
E.V.
shMAPK11
E.V. IR
shMAPK11 IR
IL-1β
p21
IL-6
IL-8
C
MCF-7
D
E
Logrank P value :
7,7·10-4
Probability
Overall Survival
Low MAPK11
High MAPK11